Hindawi
Wireless Communications and Mobile Computing
Volume 2020, Article ID 8867148, 13 pages
https://doi.org/10.1155/2020/8867148

Research Article

Security Enhancement for Energy Harvesting Cognitive Networks with Relay Selection

Khuong Ho-Van[1,2] **and Thiem Do-Dac**[1,2,3]

[1]*Ho Chi Minh City University of Technology (HCMUT), 268 Ly Thuong Kiet Street, District 10, Ho Chi Minh City, Vietnam*
[2]*Vietnam National University Ho Chi Minh City, Linh Trung Ward, Thu Duc District, Ho Chi Minh City, Vietnam*
[3]*Thu Dau Mot University, 6 Tran Van On Street, Phu Hoa Ward, Thu Dau Mot City, Binh Duong Province, Vietnam*

Correspondence should be addressed to Thiem Do-Dac; thiemdd@tdmu.edu.vn

Received 10 May 2020; Revised 1 July 2020; Accepted 29 July 2020; Published 30 September 2020

Academic Editor: Carlos T. Calafate

Relay selection is proposed in this paper as an efficient solution to secure information transmission of secondary users against eavesdroppers in energy harvesting cognitive networks. The proposed relay selection method selects a secondary relay among available secondary relays, which are capable of harvesting radio frequency energy in signals of the secondary transmitter and correctly restore secondary message, to curtail signal-to-noise ratio at the wire-tapper. In order to evaluate the security performance of the suggested relay selection method, an exact intercept outage probability formula accounting for peak transmit power confinement, Rayleigh fading, and interference power confinement is firstly derived. Monte-Carlo simulations are then generated to corroborate the proposed formula. Numerous results expose that positions of relays, the number of relays, and parameters of the energy harvesting method significantly influence the security performance while the power confinements on secondary transmitters cause the performance saturation.

1. Introduction

The explosion of emerging wireless applications, significantly increasing spectrum utilization demand, and green-and-sustainable communication induce energy efficiency and spectral efficiency to become critical design metrics for modern wireless communication networks (e.g., Fifth Generation (5G)) [1–5]. Indeed, one of the 5G system's main use cases is Internet of Things (IoT). IoT finds wide-spread applications in many fields such as electricity, transportation, military, healthcare, public safety, ... A huge number of simultaneously connected devices when deploying IoT will consume an enormous amount of energy [6]. Therefore, it is mandatory to enhance the energy efficiency so as to linger the lifetime of devices and alleviate the energy demand. Furthermore, IoT requires a wide transmission bandwidth to allocate concurrent operation of massive amount of devices. As such, in spectrum scarcity-and-shortage circumstances as nowadays [7], the problem of improving the spectral efficiency needs to be solved. Similar to IoT, meeting the increasing demand of high speed information transmission and the growing number of mobile users forces the efficient energy-and-spectrum utilization to become a mandatory design requirement for 5G mobile wireless communication systems [8].

The cognitive radio technology is an appropriate and feasible solution to improve the spectral efficiency [9]. Indeed, a cognitive radio network is decomposed into two primary and secondary subnetworks where radio frequencies are solely allotted to primary transmitters in the primary subnetwork. Nonetheless, secondary users (SUs) are also able to access the primary frequency band with interweave, overlay, and underlay mechanisms [10]. As such, the cognitive radio technology considerably enhances the spectral efficiency and overcomes the spectrum shortage problem, better fulfilling the increasing spectrum utilization demand of new wireless applications such as IoT and 5G mobile communication. In the underlay mechanism, SUs are granted access to the licensed spectrum only if SUs bound interference power induced at primary users (PUs) below an endurable threshold. SUs operating in the overlay mechanism utilize

concurrently the licensed spectrum with PUs but information transmission reliability of PUs must be maintained or improved through sophisticated coding methods. Meanwhile, the interweave mechanism solely reserves empty spectrum holes of PUs for SUs' access. Without spectrum sensing implementation for detecting the empty spectrum holes as in the interweave mechanism nor complicated coding methods as in the overlay mechanism, the underlay one is not only simple but also energy-efficient (no extra energy consumption for spectrum sensing or complicated coding). Therefore, the underlay mechanism is investigated in this paper.

Several energy efficiency improving solutions for wireless communications networks have been proposed such as network planning [11], hardware solutions [12], scavenging the energy from available sources (e.g., thermal, radio frequency (RF) powers, solar, wind, ...) [13, 14]. Among these solutions, RF signals based energy harvesting neither depends time-variant energy sources nor requires additional energy harvesting devices (e.g., wind turbines, solar panels). Such advantages which the RF signals based energy harvesting brings make it completely suitable and applicable for small-size mobile devices used in IoT or 5G mobile communication [15]. Therefore, the RF signals based energy harvesting is potential and feasible to supply the energy, prolong the operation time for wireless terminals, and increase the energy efficiency [16]. It can be implemented through Simultaneous Wireless Power and Information Transfer [17–19] or relaying communication [20–22]. Moreover, RF signals based energy harvesting circuits were successfully designed and tested [23, 24].

Energy harvesting cognitive networks (EHCNs) combine two emerging technologies (cognitive radio and RF energy harvesting). Therefore, EHCNs are expected to achieve multiple design criteria of modern wireless communication networks (e.g., 5G), such as high spectral and energy efficiencies [25–27]. However, EHCNs allow both secondary and primary users to utilize the licensed spectrum concurrently. As such, information security in these networks is of great concern. For information security against wire-tappers, physical layer security (PLS) has lately been suggested as a complementary-and-cheap measure to the traditional encryption and cryptographic techniques [28]. Various techniques, such as transmit beam-forming [29], opportunistic scheduling [30], transmit antenna selection [31], jamming [32], on-off transmission [33], and relaying [34], can be applied for PLS. Among them, the relay selection has received considerable attentions because of the following reasons. Firstly, the relay selection achieves higher spectral efficiency than all-relay transmission while the benefits of all-relay transmission, such as diversity order and coding gain, are still maintained for the relay selection [35]. Secondly, the relay selection sustains the secondary transmitter-destination connection through relaying in case that this connection is blocked owing to heavy shadowing or severe fading or the limited transmission range of SUs (It is recalled that the underlay mechanism allocates the transmit power of SUs, which limits the radio coverage of SUs.). Finally, the relay can be selectively-and-purposely chosen in order to not only disrupt the eavesdroppers' signal reception but also enhance the reliability of received signals at the desired destination. The current paper suggests a relay selection method with the objective of minimizing the overhearing of the eavesdroppers in EHCNs where all relays are self-powered with harvesting radio frequency energy in signals of the secondary transmitter and the transmit powers of all SUs are limited by the peak interference power as well as the peak transmit power.

1.1. Related Works. This subsection solely surveys works pertaining to the relay selection in EHCNs for secure information transmission against eavesdroppers. More specifically, this review relied on notable characteristics (Existing works (e.g., [36–40]), which did not reflect these characteristics, should not be reviewed. For example, [36–38] considered non-cognitive radio networks with energy harvesting; [39, 40] provided the security capability analysis of the relay selection in cognitive radio networks without energy harvesting.) including the relay selection, security performance analysis, the interference power confinement, the energy harvesting, the peak transmit power confinement, the underlay mechanism. Through this survey, our contributions are summarized in successive subsection. Actually, only few works mentioned the relay/path selection in EHCNs for secure information transmission against eavesdroppers. More specifically, the most relevant work is [41] in which the relay selection follows two steps: the successfully decoding set that consists of relays exactly recovering the secondary message is first formed and then the relay (in the successfully decoding set) which creates the largest signal-to-noise ratio (SNR) at the secondary destination is chosen. All secondary relays are self-powered with harvesting radio frequency energy in signals of the secondary transmitter through the time-switching (TS) method [42] where one complete secondary transmitter-to-destination transmission undergoes three phases: energy harvesting at relays, information transmission of the secondary transmitter, and information transmission of the selected relay. Both (peak transmit and interference) power confinements regulate power distribution for the relays and the secondary transmitter. Nevertheless, [41] only provides simulation results on the secrecy outage probability (SOP) of the investigated relay selection in EHCNs. The relatively relevant work is [43] where the path selection, instead of the relay selection as [41], was proposed for multi-hop multi-path EHCNs in which multiple paths, each consisting of multiple hops, connect the secondary transmitter with the secondary destination. Only one path providing the largest SNR is adopted to maintain secondary transmitter-destination connection. In [43], all SUs collect the energy from dedicated beacons through the TS method and their transmit powers are subject to the peak transmit power confinement, the condition that the eavesdropper fails to recover SUs' message, and the interference power confinement. The outage possibility at the secondary destination was analyzed in an accurate closed form under the assumption of all statistically independent end-to-end SNRs of transmission paths. This assumption is not always correct since the transmit power of the secondary transmitter is a common term which appears in all end-to-end SNRs of transmission paths; hence, these end-to-end SNRs are correlated in general.

1.2. Motivation and Contributions. Although the relay selection has several advantages, rare attention has been paid on the relay selection in EHCNs for PLS. This motivates us to further study it in order to have a complete evaluation on many aspects (information security, spectral efficiency, energy efficiency, secondary transmitter-destination connection probability) of EHCNs before practical deployment. This paper reconsiders the system model in [41] but with the below distinctions:

(i) Our paper suggests a different relay selection method in which the chosen relay from the successfully decoding set is the one which minimizes the SNR at the eavesdropper. This prevents the eavesdropper from decoding legitimate information as much as possible

(ii) All relays in this paper harvest the energy with the power splitting (PS) method which differs the TS method in [41].

(iii) This paper analyzes the intercept outage probability (IOP) in an exact form while [41] merely supplied simulation results of the SOP

Our contributions are briefly listed as:

(i) Suggest a relay selection method in EHCNs to hinder the eavesdropper from overhearing as much as possible

(ii) Derive an exact IOP formula for quickly assessing the security measure of the suggested relay selection method in EHCNs under Rayleigh fading channels and the (peak transmit and interference) power confinements

(iii) Prove the existence of optimum key system parameters for the best security performance

(iv) Provide insightful results on the security performance: *i*) IOP is saturated when the peak transmit power of the secondary transmitter is large; *ii*) security performance is significantly enhanced with appropriate selections of relays' positions, information relaying and energy harvesting times, and power partition for energy harvesting and information decoding

1.3. Outline. This paper continues with channel and system models in Part II. Then, Part III derives the IOP in detail. Illustrative results and conclusions are delivered in Part IV and Part V, correspondingly.

1.4. Notations. $c \sim \mathcal{CN}(0, \eta)$ denotes the circularly symmetric complex Gaussian random variable c with η variance and zero mean; $f_{\mathscr{V}}(x)$ and $F_{\mathscr{V}}(x)$ are the probability density function (PDF) and the cumulative distribution function (CDF) of the random variable $\mathscr{V}$, correspondingly; $\Pr\{\mathscr{V}\}$ denotes the possibility of the event $\mathscr{V}$; $\Pr\{\mathscr{V}|\mathscr{M}\}$ is the probability of the event $\mathscr{V}$ conditioned on $\mathscr{M}$; $\binom{n}{k} = n!/k!(n-k)!$ is the binomial coefficient; $\Xi_Y\{\cdot\}$ stands for the expectation with respect to (w.r.t) the random variable Y; $|\mathscr{V}|$ denotes the size of the set $\mathscr{V}$.

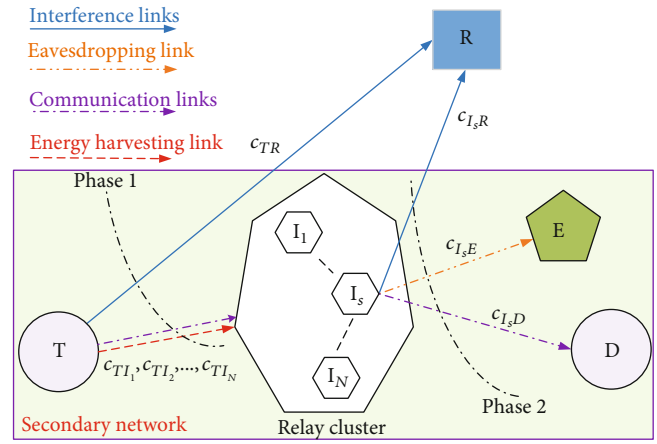

FIGURE 1: System model.

2. System and Channel Models

Figure 1 considers the relay selection in EHCNs where the secondary transmitter T communicates the secondary destination D. The secondary message, which is transmitted by T, is illegally extracted by an eavesdropper E. Because of severe fading and heavy shadowing, direct communication between T and D and between T and E may be unavailable. Accordingly, the current paper suggests to choose a relay I_s from a cluster of N relays (I_1, I_2, ..., I_N) between T and D for two purposes: *i*) maintain communication between T and D through relaying; *ii*) limit the eavesdropping of E. For the underlay mechanism under consideration, T and I_r with $r \in [1, N]$ interfere the signal reception at the primary receiver R. This paper assumes (This assumption is commonly accepted in cognitive radio related publications (e.g. [44–46]).) that primary transmitters are far away from D, E and I_r with $r \in [1, N]$ or interferences from primary transmitters are Gaussian-distributed. As such, interferences from primary transmitters are neglected or incorporated into noise terms at corresponding secondary receivers. Moreover, this paper assumes that T is not power-constrained. Therefore, relays with limited power can scavenge the energy in RF signals of T.

In Figure 2(a), β is the time for the secondary message to reach D, which is partitioned into two phases. The Phase 1, which remains $\varepsilon\beta$ where the time splitting ratio is denoted as $\varepsilon \in (0, 1)$, is for T to send the secondary message based on which relays harvest the energy with the power splitting method (e.g., [47, 48]) and decode the secondary message as exposed in Figure 2(b). This method splits the received signal of I_r into two fractions: one fraction $\sqrt{\omega}o_{TI_r}$ for decoding the secondary message (The message decoder is assumed to spend neglected energy. This assumption is popularly accepted in open literature (e.g., [49–55]).) and the other fraction $\sqrt{1-\omega}o_{TI_r}$ for harvesting the energy, where o_{TI_r} is the received signal of I_r and $\omega \in (0, 1)$ is the power splitting

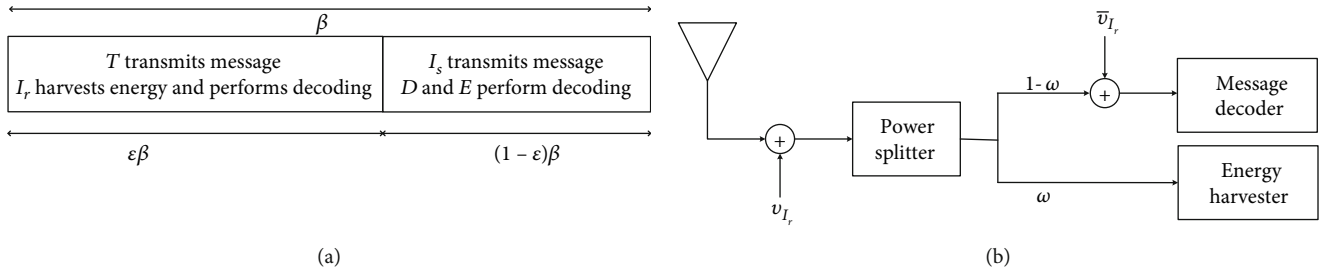

FIGURE 2: Message processing at I_r and phase times. (a) Phase times, (b) Message processing at Ir.

ratio. The Phase 1 ends with the relay selection as follows. First, Δ, which denotes a set of relays that exactly recover the secondary message, is formed. Then, the relay I_s in Δ, which creates the smallest SNR at E, is selected (This paper assumes that each relay can obtain the channel state information (CSI) of channels from and to it (i.e., I_r -E channel, I_r -D channel, and T-I_r channel) such that the SNRs of these channels are available at it [56–58]. Such CSI can be estimated, for example, through the exchange of clear-to-send signal and ready-to-send signal between D and I_r and between T and I_r [59], and through local oscillator power leakage from the wire-tapper's radio frequency front-end [60, 61]. Furthermore, the relay selection method in this paper can be carried out in a distributed manner, for instance, using the timer concept where the relay I_r in Δ sets the value of its timer which is proportional to the SNR of the I_r-E channel. Therefore, the relay whose timer runs out first is selected.). Such a relay selection is to reduce the successful decoding probability of E. The Phase 2, which remains $(1-\varepsilon)\beta$, is for the chosen relay I*s* to re-encode the decoded secondary message and broadcast the re-encoded message to D and E.

In Figure 1, $c_{\mathtt{jk}}$, $\mathtt{j} \in \{T, I_1, I_2, ..., I_N\}$ and $\mathtt{k} \in \{I_1, I_2, ..., I_N, E, D, R\}$, signifies the $\mathtt{j}$-$\mathtt{k}$ channel coefficient. The current paper models $c_{\mathtt{jk}} \sim \mathcal{CN}(0, \eta_{\mathtt{jk}})$. Such a model of $c_{\mathtt{jk}}$ implies that wireless channels under consideration are Rayleigh-distributed. With incorporating path-loss, $\eta_{\mathtt{jk}}$ is represented as $\eta_{\mathtt{jk}} = d_{\mathtt{jk}}^{-\zeta}$ where $d_{\mathtt{jk}}$ refers the $\mathtt{j}$-$\mathtt{k}$ distance and ζ denotes the path-loss exponent. Then, the PDF and the CDF of the channel gain $g_{\mathtt{jk}} = |c_{\mathtt{jk}}|^2$ are correspondingly expressed as $f_{g_{\mathtt{jk}}}(x) = e^{-x/\eta_{\mathtt{jk}}}/\eta_{\mathtt{jk}}$ and $F_{g_{\mathtt{jk}}}(x) = 1 - e^{-x/\eta_{\mathtt{jk}}}$, where $x \geq 0$.

The relay I_r receives the following signal in the Phase 1:

$$o_{TI_r} = c_{TI_r}\sqrt{P_T} i_T + \upsilon_{I_r}, \tag{1}$$

where i_T is the unit power symbol sent by T, P_T is the transmit power of T, and $\upsilon_{I_r} \sim \mathcal{CN}(0, V_{I_r})$ is the receiver noise at I_r. Without loss of generality and for notation simplicity, equal noise variances at relays' receivers are assumed (i.e., $V_{I_r} = V_I$, $\forall r \in [1, N]$).

The T's transmit power, P_T, must be established in the underlay mechanism as [62].

$$P_T = \min\left(\frac{Q_p}{g_{TR}}, P_p\right), \tag{2}$$

for controlling the interference power induced at R within a bearable level, upper-bounding the transmit power of T by the peak transmit power P_p restricted by hardware implementation, and maximizing the transmission range of T. Here, Q_p is the peak interference power agonized by R.

According to Figure 2(b), I_r harvests the sum energy in the Phase 1 as

$$E_{I_r} = \varphi\omega\left(P_T g_{TI_r} + V_I\right)\varepsilon\beta, \tag{3}$$

where the energy conversion efficiency is $\varphi \in (0, 1)$. Accordingly, the peak power which the relay I_r can transmit signals in the Phase 2 is

$$P_{I_r} = \frac{E_{I_r}}{(1-\varepsilon)\beta} = P_T g_{TI_r} M + L, \tag{4}$$

in which

$$M = \varepsilon\varphi\omega/(1-\varepsilon), \tag{5}$$

$$L = V_I M. \tag{6}$$

Figure 2(b) shows that the input signal of the message decoder of the relay I_r is

$$\bar{o}_{TI_r} = \sqrt{1-\omega}\, o_{TI_r} + \bar{\upsilon}_{I_r}, \tag{7}$$

where $\bar{\upsilon}_{I_r} \sim \mathcal{CN}(0, \bar{V}_{I_r})$ is the noise generated by the passband-to-baseband signal conversion. Without loss of generality, equal noise variances at the passband-to-baseband signal converters are assumed (i.e., $\bar{V}_{I_r} = \bar{V}_I$, $\forall r \in [1, N]$).

Plugging (1) into (7) results in

$$\bar{o}_{TI_r} = \sqrt{(1-\omega)P_T} c_{TI_r} i_T + \sqrt{1-\omega}\upsilon_{I_r} + \bar{\upsilon}_{I_r}. \tag{8}$$

It is inferred from (8) that the message decoder of the relay I_r obtains the input SNR as

$$\Upsilon_{TI_r} = \frac{P_T g_{TI_r}}{\hat{V}_I}, \tag{9}$$

where

$$\widehat{V}_I = V_I + \frac{\bar{V}_I}{1-\omega}. \tag{10}$$

The channel capacity that the relay I_r can obtain is $C_{TI_r} = \varepsilon \log_2(1 + \Upsilon_{TI_r})$ bps/Hz where ε preceding the logarithm is because the Phase 1 remains $\varepsilon\beta$. Based on the communication theory, I_r correctly restores the secondary message only if its channel capacity is above the target transmission rate C_t, i.e., $C_{TI_r} \geq C_t$. In other words, i_T is successfully restored at I_r if $\Upsilon_{TI_r} \geq \Upsilon_t$ where $\Upsilon_t = 2^{C_t/\varepsilon} - 1$.

The Phase 1 ends by grouping relays which exactly restore the secondary message into a set Δ as

$$\Delta = \left\{ \mathtt{I}_r : Y_{TI_r} \geq Y_t,\ r \in [1, N] \right\}. \tag{11}$$

Then, the relay in Δ which minimizes the SNR at E is chosen (It is noted that [38] proposed the same relay selection method as ours. Nonetheless, [38] considered the non-cognitive scenario while our paper investigated the cognitive scenario. As such, the analysis in our paper differs that in [38].). In other words, the selected relay can be mathematically represented as

$$\mathtt{I}_s = \arg \min_{\mathtt{I}_r \in \Delta} \Upsilon_{I_rE}, \tag{12}$$

where Υ_{I_rE} is the SNR at E through the $I_r - E$ channel.

Such a relay selection in (12) apparently boosts the IOP at E, improving the security capability.

The Phase 2 is for I_s to broadcast the decoded message i_{I_s}. As such, E receives the signal in the Phase 2 as

$$o_{I_sE} = c_{I_sE}\sqrt{\bar{P}_{I_s}}\, i_{I_s} + \upsilon_E, \tag{13}$$

in which $\bar{P}_{I_s}$ is the transmit power of I_s and $\upsilon_E \sim \mathcal{CN}(0, V_E)$ is the receiver noise at E.

E obtains the following SNR in the Phase 2, which is computed from (13), as

$$\Upsilon_{I_sE} = \frac{g_{I_sE}\bar{P}_{I_s}}{V_E}. \tag{14}$$

Generally, the SNR at E through the $I_r - E$ channel is derived in a similar manner to (14), i.e.,

$$\Upsilon_{I_rE} = \frac{g_{I_rE}\bar{P}_{I_r}}{V_E}, \tag{15}$$

where the transmit power of I_r is $\bar{P}_{I_r}$.

I_r allocates its transmit power according to the underlay mechanism as

$$\bar{P}_{I_r} = \min\left(\frac{Q_p}{g_{I_rR}}, P_{I_r}\right), \tag{16}$$

which is similar to (2).

The channel capacity at E in the Phase 2 is given by

$$C_{I_sE} = (1-\varepsilon)\log_2\left(1 + \Upsilon_{I_sE}\right), \tag{17}$$

where $(1-\varepsilon)$ preceding the logarithm is because the Phase 2 remains $(1-\varepsilon)\beta$.

3. Intercept Outage Probability Analysis

The IOP is the possibility which the wire-tapper E fails to decode the secondary message. As such, it is a critical performance indicator to assess the security capability of the relay selection in EHCNs. This section proposes an exact IOP formula for quickly measuring the secrecy performance without invoking exhaustive simulations.

The IOP is defined as

$$\Theta = \Pr\left\{C_{I_sE} \leq C_t\right\}, \tag{18}$$

where C_t is the target transmission rate.

Inserting (17) into (18) results in

$$\Theta = \Pr\left\{(1-\varepsilon)\log_2\left(1 + \Upsilon_{I_sE}\right) \leq C_t\right\} = \Pr\left\{\Upsilon_{I_sE} \leq \Upsilon_e\right\}, \tag{19}$$

where $\Upsilon_e = 2^{C_t/(1-\varepsilon)} - 1$.

It is recalled that I_s is the relay in the set Δ providing the smallest SNR at E. Therefore, Υ_{I_sE} can be represented in terms of Υ_{I_rE} with $\mathtt{I}_r \in \Delta$ as

$$\Upsilon_{I_sE} = \min_{\mathtt{I}_r \in \Delta} \Upsilon_{I_rE} \tag{20}$$

Additionally, the formation of the set Δ implicitly means that the relays in Δ (i.e., $\mathtt{I}_r \in \Delta$) successfully restore the secondary message (i.e., $\Upsilon_{TI_r} \geq \Upsilon_t$) while the relays not in Δ (i.e., $\mathtt{I}_k \in \bar{\Delta}$) fail to recover the secondary message (i.e., $\Upsilon_{TI_k} < \Upsilon_t$). By denoting $|\Delta|$ and $|\bar{\Delta}|$ as the sizes of Δ and $\bar{\Delta}$, respectively, it is inferred that $|\Delta| + |\bar{\Delta}| = N$. Therefore, (19) can be explicitly rewritten as

$$\Theta = \Pr\left\{\min_{\mathtt{I}_r \in \Delta} \Upsilon_{I_rE} \leq \Upsilon_e, \bigcap_{\mathtt{I}_r \in \Delta}\left\{\Upsilon_{TI_r} \geq \Upsilon_t\right\}, \bigcap_{\mathtt{I}_k \in \bar{\Delta}}\left\{\Upsilon_{TI_k} < \Upsilon_t\right\}\right\}. \tag{21}$$

Because $|\Delta| = 0$ falls in the range of $[0, N]$, (21) is

further rewritten according to the law of total probability as

$$\Theta = \sum_{|\Delta|=0}^{N} \sum_{\Delta} \Pr\left\{ \min_{\mathtt{I}_r \in \Delta} \Upsilon_{I_r E} \le \Upsilon_e, \bigcap_{\mathtt{I}_r \in \Delta} \left\{ \Upsilon_{TI_r} \ge \Upsilon_t \right\}, \bigcap_{\mathtt{I}_k \in \bar{\Delta}} \left\{ \Upsilon_{TI_k} < \Upsilon_t \right\} \right\}. \tag{22}$$

Since $|\Delta| = 0$ corresponds to the case which no relay exactly restores the secondary message, the event $\min_{\mathtt{I}_r \in \Delta} \Upsilon_{I_r E} \le \Upsilon_e$ with $|\Delta| = 0$ always happens with the probability of 1. Therefore, the term in (22) corresponding to $|\Delta| = 0$ can be expressed as

$$\mathscr{R} = \Pr\left\{ \Upsilon_{TI_1} \le \Upsilon_t, \Upsilon_{TI_2} \le \Upsilon_t, \cdots, \Upsilon_{TI_N} \le \Upsilon_t \right\}. \tag{23}$$

Without loss of generality, the current paper assumes that relays are closely located (i.e., $\eta_{TI_r} = \eta_{TI}$, $\eta_{I_r D} = \eta_{ID}$, $\eta_{I_r R} = \eta_{IR}$, $\eta_{I_r E} = \eta_{IE}$, $\forall r \in [1, N]$) for analysis tractability. As such, if $|\Delta| = \mathtt{m}$ is fixed, then $\Pr\{\min_{\mathtt{I}_r \in \Delta} \Upsilon_{I_r E} \le \Upsilon_e, \bigcap_{\mathtt{I}_r \in \Delta} \{ \Upsilon_{TI_r} \ge \Upsilon_t \}, \bigcap_{\mathtt{I}_k \in \bar{\Delta}} \{ \Upsilon_{TI_k} < \Upsilon_t \}\}$ is independent of elements forming the set Δ. Moreover, the total number of sets, each with $|\Delta| = \mathtt{m}$ elements, is $\binom{N}{\mathtt{m}}$. Therefore, (22) is simplified as

$$\begin{aligned} \Theta &= \mathscr{R} + \sum_{|\Delta|=1}^{N} \binom{N}{|\Delta|} \Pr\left\{ \min_{\mathtt{I}_r \in \Delta} \Upsilon_{I_r E} \le \Upsilon_e, \bigcap_{\mathtt{I}_r \in \Delta} \left\{ \Upsilon_{TI_r} \ge \Upsilon_t \right\}, \bigcap_{\mathtt{I}_k \in \bar{\Delta}} \left\{ \Upsilon_{TI_k} < \Upsilon_t \right\} \right\} \\ &= \mathscr{R} + \sum_{|\Delta|=1}^{N} \binom{N}{|\Delta|} \underbrace{\Xi_{P_T} \left\{ \underbrace{\Pr\left\{ \min \Upsilon_{I_r E} \le \Upsilon_e, \cap \left\{ \Upsilon_{TI_r} \ge \Upsilon_t \right\}, \cap \left\{ \Upsilon_{TI_k} < \Upsilon_t \right\} \middle| P_T \right\}}_{\mathscr{H}} \right\}}_{\mathscr{W}}. \end{aligned} \tag{24}$$

Now, two terms of (24) are computed to finish the derivation of Θ.

Theorem 1. *$\mathscr{R}$ is expressed in an accurate closed form as*

$$\mathscr{R} = \sum_{l=0}^{N} \binom{N}{l} (-1)^l \left(\frac{1-B}{B} e^{-AB/\eta_{TR}} + e^{-G} \right) \tag{25}$$

where

$$A = \frac{Q_p}{P_p}, \tag{26}$$

$$B = \frac{\eta_{TR} \Upsilon_t \widehat{V}_I l}{\eta_{TI} Q_p} + 1, \tag{27}$$

$$G = \frac{\Upsilon_t \widehat{V}_I l}{\eta_{TI} P_p}. \tag{28}$$

Proof. Please see Appendix A.

Theorem 2. *$\mathscr{W}$ is derived in a precise form as*

$$\begin{aligned} \mathscr{W} = \int_0^{\infty} &\left[e^{-K|\Delta|/\min\left(\frac{Q_p}{x}, P_p\right)} - \left\{ (S-1) \mathscr{K}\left(U, \min\left(\frac{Q_p}{x}, P_p \right) \right) + \mathscr{K}\left(H, \min\left(\frac{Q_p}{x}, P_p \right) \right) \right\}^{|\Delta|} \right] \\ &\times \left(1 - e^{-K/\min\left(\frac{Q_p}{x}, P_p\right)} \right)^{N-|\Delta|} \frac{1}{\eta_{TR}} e^{-x/\eta_{TR}} dx, \end{aligned} \tag{29}$$

where $\mathbf{W}_{x,\,y}(z)$ is the Whittaker function [63], eq. (1087.4) built in computational tools (e.g., Mathematica, Matlab) and

$$K = \frac{\Upsilon_t \widehat{V}_I}{\eta_{TI}}, \tag{30}$$

$$U = \frac{\Upsilon_e V_E}{\eta_{IE}} + \frac{Q_p}{\eta_{IR}}, \tag{31}$$

$$S = \frac{Q_p}{\eta_{IR} U}, \tag{32}$$

$$H = \frac{\Upsilon_e V_E}{\eta_{IE}}, \tag{33}$$

$$\mathcal{G}(c, v, b) = \sum_{m=0}^{\infty} \frac{(-vb)^m}{m!b} (cb)^{-m/2} e^{-cb/2} \mathbf{W}_{-m/2,1-m/2}(cb), \tag{34}$$

$$\mathcal{K}(n, P_T) = \frac{e^{L/\eta_{TI} P_T M}}{\eta_{TI}} \mathcal{G}\left(\frac{\Upsilon_t \hat{V}_I + L/M}{P_T}, \frac{n}{P_T M}, \frac{1}{\eta_{TI}}\right). \tag{35}$$

Proof. Please see Appendix B.

Inserting (25) and (29) into (24), one obtains the exact IOP formula for the proposed relay selection in EHCNs in a single-integral form as

$$\Theta = \mathcal{R} + \sum_{|\Delta|=1}^{N} \binom{N}{|\Delta|} \mathcal{W} \tag{36}$$

It is well-known that the single integral in (36) can be solved by numerical methods available in computational tools (e.g., Matlab, Mathematica). Accordingly, the accurate IOP formula in (36) for the proposed relay selection in EHCNs considering both the (peak transmit and interference) power confinements can be straightforwardly computed, which is useful to promptly measure the secrecy performance without time-consuming simulations. Relied on our understanding, this formula has not been published yet.

4. Results and Discussions

The IOP of the proposed relay selection in EHCNs is evaluated through critical system parameters. For illustration purposes, some specifications are selected as follows: T at (0.0, 0.0), I_r at (d, 0.0), D at (1.0, 0.0), E at (0.9, 0.5), R at (0.4, 0.6), C_t =0.1 bps/Hz, $\varphi = 0.9$, $V_E = V_I = \bar{V}_I = N_0$, $\zeta = 3$. In the sequel, "The." means the theoretical result in (36) whereas "Sim." implies the simulated result.

Figure 3 shows the IOP w.r.t P_p/N_0 for ω=0.7, ε=0.6, d=0.4, Q_p/N_0=15 dB. The results illustrate that the simulation coincides with the theory, verifying the preciseness of (36). Additionally, the IOP decreases with increasing P_p/N_0. This comes from the fact that increasing P_p/N_0 allows the relays to exactly restore the secondary message and to scavenge more radio frequency energy in signals of T, hence increasing the SNR at E in the Phase 2 and reducing the IOP. Nevertheless, the IOP bears the error floor at large P_p/N_0. This error floor is because of the power allocation for secondary transmitters (please recall (2) and (16)) where large values of P_p/N_0 make the transmit powers of T and I_r independent of P_p/N_0 (i.e., large P_p/N_0 neglects the peak transmit power confinement), inducing the constant IOP. Moreover, the IOP is proportional to the number of relays, confirming the effectiveness of the relay selection in improving the secrecy performance.

Figure 4 demonstrates the IOP w.r.t Q_p/N_0, with parameters of Figure 3, excepting P_p/N_0=10 dB. The results expose that the theory coincides the simulation, again proving the validity of (36). Additionally, the IOP declines with Q_p/N_0. This result is comprehended from the power distribution of T and I_r, similarly to Figure 3. Moreover, the IOP increases with the number of relays, showing the importance of the proposed relay selection method in preventing the wiretapper from overhearing the secondary message.

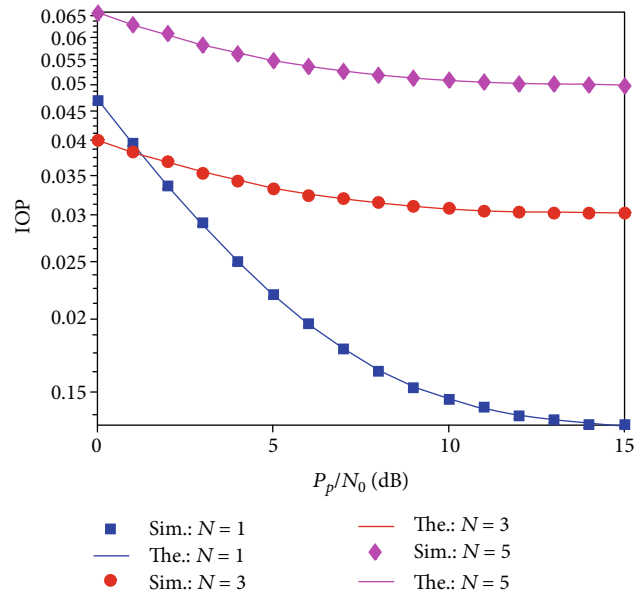

Figure 3: IOP w.r.t P_p/N_0.

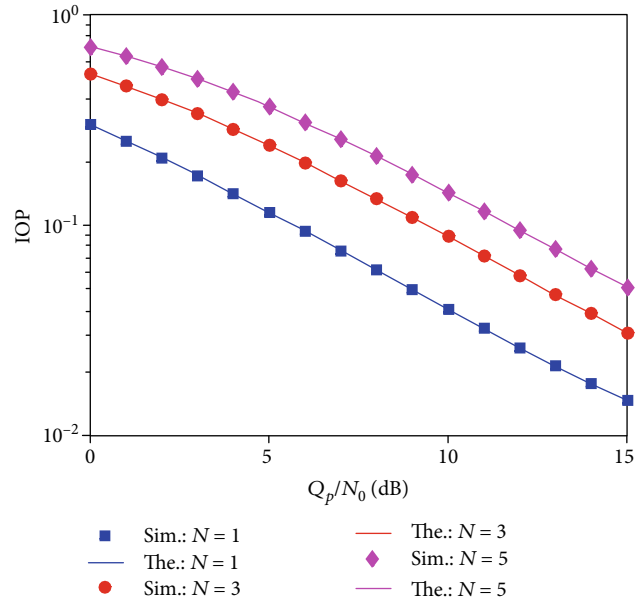

Figure 4: IOP w.r.t Q_p/N_0.

Figure 5 exposes the IOP w.r.t the distance from T to the relay group, with parameters of Figure 4, excepting P_p/N_0=16 dB and Q_p/N_0=12 dB. The results prove that the theory agrees with the simulation, again asserting the accuracy of (36). It should be reminded that the intercept outage event happens as the set Δ does not exist (i.e., the relay group is distant from T) or the selected relay I_s in the set Δ cannot

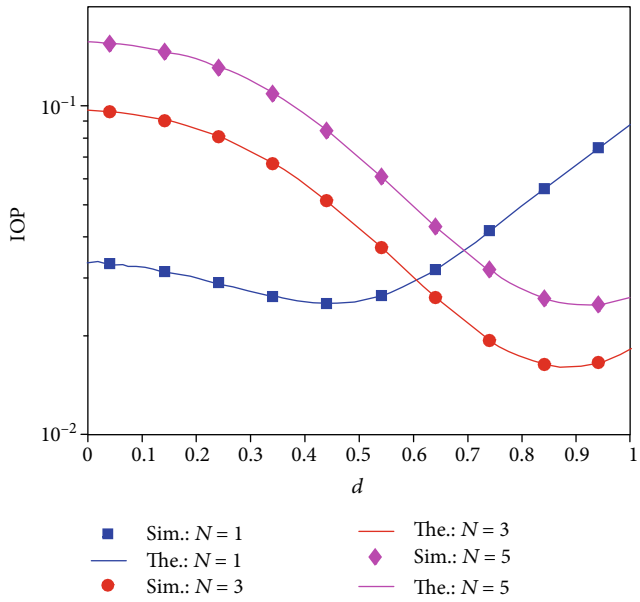

Figure 5: IOP w.r.t d.

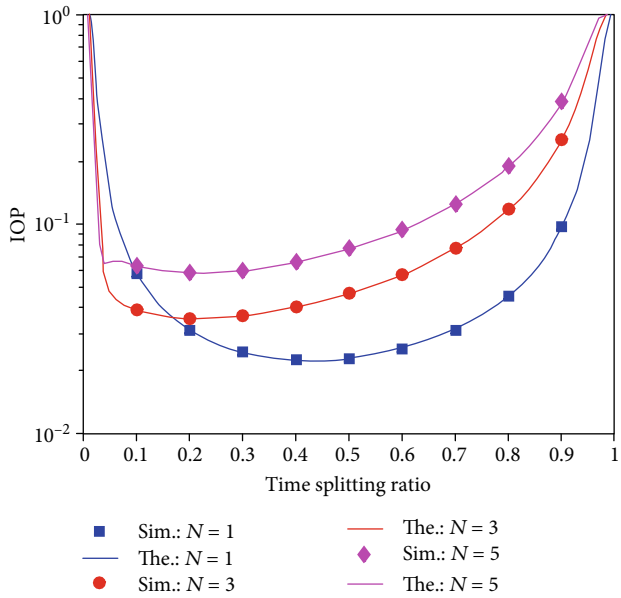

Figure 6: IOP w.r.t ε.

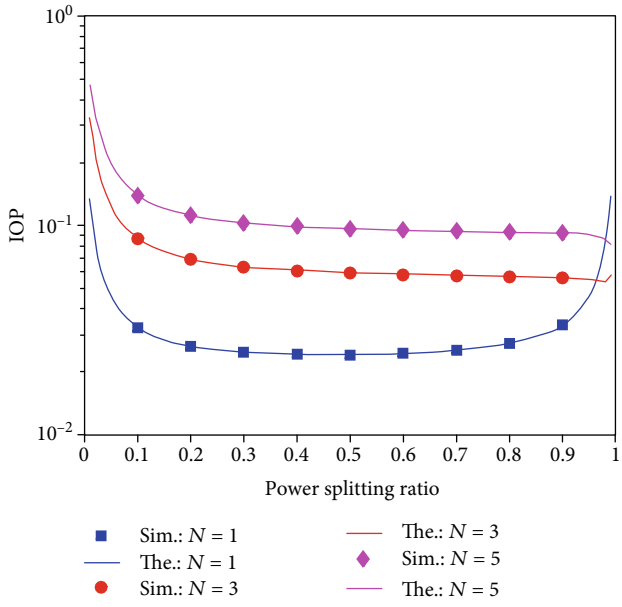

Figure 7: IOP w.r.t ω.

create the sufficient SNR at E (i.e., the relay group is distant from E). As such, the least secured information transmission (i.e., the IOP is minimum) happens when the relay group is located in a convenient position for E to eavesdrop the largest amount of information. This convenient position apparently represents the best compromise between the probability that the set Δ exists and the probability that E can achieve the highest SNR from the selected relay. Figure 5 shows that the least secure information transmission happens at d_{worst}=0.44, 0.88, 0.92 for N=1, 3, 5, respectively. That the d_{worst} is proportional to N can be interpreted as follows: *i*) The probability that the set Δ exists is higher for the larger value of N; hence, the relay group can be placed more distantly from T (i.e., increase d) as N increases; *ii*) That the relay group can be placed more distantly from T for the larger value of N induces the selected relay in Δ to be closer to E; hence, the SNR at E is improved and the IOP is reduced. Furthermore, Figure 5 apparently demonstrates the efficacy of the proposed relay selection (i.e., the IOP decreases with increasing N) in EHCNs.

Figure 6 plots the IOP w.r.t the time splitting ratio ε, with parameters of Figure 5, excepting d=0.4. The results expose that the theory coincides with the simulation, asserting the preciseness of (36). Moreover, the secrecy performance is better with the larger number of relays due to having more chances to select the optimum relay. Figure 6 exactly reflects this comment since increasing N induces an increase in the IOP. Furthermore, the time splitting ratio impacts the amount of the harvested energy and the relays' probability of successfully decoding the secondary message in the Phase 1 and the channel capacity at E in the Phase 2. More specifically, increasing ε prolongs the time of the Phase 1; therefore, the relays can scavenge more energy and accurately restore the secondary message with a larger probability. Nonetheless, increasing ε reduces the time of the Phase 2; hence, the channel capacity at E decreases and the IOP increases. Therefore, it is expected that there exists a certain value of ε that makes the IOP minimized (equivalently, the worst security performance). Figure 6 apparently illustrates this observation. To be more specific, the minimum IOPs happen at ε_{worst}=0.41, 0.22, 0.21 for N=1, 3, 5, respectively.

Figure 7 exposes the IOP w.r.t the power splitting ratio ω, with parameters of Figure 6, excepting ε=0.6. The results illustrate that the theory coincides the simulation, proving the preciseness of (36). Additionally, the larger number of relays drastically increases the IOP, demonstrating the efficacy of the suggested relay selection in reducing the information eavesdropping of E. Furthermore, turning appropriately the power splitting ratio can avoid the degradation of the

security performance. For example, ω should not be chosen in the range of [0.2, 0.7] for $N=1$ in which the IOP is small (i.e., bad security performance). This is because increasing ω enables the relays to harvest more energy; thus, the relays can produce high SNRs at E, eventually declining the IOP. Nonetheless, increasing ω also decreases the energy reserved for the message decoder, which consequently reduces the size of Δ (i.e., reducing the chance to adopt the optimum relay for minimizing the SNR at E) and increases the IOP. Therefore, appropriate selection of ω can avoid the least secure information transmission (i.e., smallest IOP). In Figure 7, the smallest IOP happens at $\omega=0.41$ for $N=1$.

5. Conclusion

This paper proposes the relay selection method to improve the information security in energy harvesting cognitive networks against eavesdroppers. The relays are able to harvest radio frequency energy in the signals of the power-unconstrained secondary transmitter and the relay which creates the smallest SNR at the eavesdropper is adopted to decode and forward the secondary message to the secondary destination. The security performance of the proposed relay selection method considering both (peak transmit and interference) power confinements and Rayleigh distribution is quickly measured by the suggested precise IOP formula that is asserted by Monte-Carlo simulations. Multiple results indicate that the positions of the relays and the parameters (power and time splitting ratios) of the energy harvesting method can be properly adjusted to increase the IOP, eventually improving the security performance. Moreover, the IOP experiences the error floor as the transmit power is high.

Appendix

A. Proof of THEOREM 1

$\mathscr{R}$ in (23) is explicitly expressed as

$$\mathscr{R} = \Xi_{P_T}\left\{\Pr\left\{\Upsilon_{TI_1} \le \Upsilon_t, \Upsilon_{TI_2} \le \Upsilon_t, \cdots, \Upsilon_{TI_N} \le \Upsilon_t \middle| P_T\right\}\right\}. \tag{A.1}$$

Conditioned on P_T, the events $\{\Upsilon_{TI_r} \le \Upsilon_t\}$ with $r \in [1, N]$ are uncorrelated. Additionally, that relays are closely located induces $\Pr\{\Upsilon_{TI_1} \le \Upsilon_t | P_T\} = \Pr\{\Upsilon_{TI_2} \le \Upsilon_t | P_T\} = \cdots = \Pr\{\Upsilon_{TI_N} \le \Upsilon_t | P_T\} = \mathscr{Z}$. Equivalently, $\Pr\{\Upsilon_{TI_r} \le \Upsilon_t | P_T\}$ is the same for any relay I_r. Therefore, (A.1) is simplified as

$$\mathscr{R} = \Xi_{P_T}\left\{\underbrace{\left(\Pr\left\{\Upsilon_{TI_r} \le \Upsilon_t \middle| P_T\right\}\right)}_{\mathscr{Z}}^{N}\right\}. \tag{A.2}$$

Using (9), one can rewrite $\mathscr{Z}$ as

$$\mathscr{Z} = \Pr\left\{\frac{P_T g_{TI_r}}{\widehat{V}_I} \le \Upsilon_t \middle| P_T\right\}. \tag{A.3}$$

It is recalled that $\eta_{TI_r} = \Xi_{g_{TI_r}}\{g_{TI_r}\} = \eta_{TI}$. Therefore, (A.3) is further simplified as

$$\mathscr{Z} = \Pr\left\{g_{TI_r} \le \frac{\Upsilon_t \widehat{V}_I}{P_T}\right\} = 1 - e^{-\Upsilon_t V \wedge_I / P_T \eta_{TI}}. \tag{A.4}$$

Inserting (A.4) into (A.2) and using $P_T = \min((Q_p/g_{TR}), P_p)$ in (2), the expectation with respect to P_T is solved as

$$\begin{aligned}\mathscr{R} &= \Xi_{P_T}\left\{\left(1 - e^{-\Upsilon_t V \wedge_I / P_T \eta_{TI}}\right)^N\right\} \\ &= \sum_{l=0}^{N} \binom{N}{l} (-1)^l \Xi_{P_T}\left\{e^{-\Upsilon_t V \wedge_I l / P_T \eta_{TI}}\right\} \\ &= \sum_{l=0}^{N} \binom{N}{l} (-1)^l \left(\int_{Q_p/P_p}^{\infty} e^{-\Upsilon_t V \wedge_I l / \eta_{TI} Q_p x} \frac{1}{\eta_{TR}} e^{-x/\eta_{TR}} dx \right. \\ &\quad \left. + \int_{0}^{Q_p/P_p} e^{-\Upsilon_t V \wedge_I l / \eta_{TI} P_p} \frac{1}{\eta_{TR}} e^{-x/\eta_{TR}} dx\right)\end{aligned} \tag{A.5}$$

The above integrals are straightforwardly computed; hence, $\mathscr{R}$ in (A.5) exactly matches (25) after using new notations in (26), (27), (28). This finishes the proof.

B. Proof of THEOREM 2

Conditioned on P_T, the event $\{\min_{I_r \in \Delta} \Upsilon_{I_r E} \le \Upsilon_e, \cap_{I_r \in \Delta} \{\Upsilon_{TI_r} \ge \Upsilon_t\}\}$ is independent of the event $\{\cap_{I_k \in \bar{\Delta}} \{\Upsilon_{TI_k} < \Upsilon_t\}\}$. Therefore, the term $\mathscr{H}$ in $\mathscr{W}$ is decomposed as

$$\mathscr{H} = \underbrace{\Pr\left\{\min \Upsilon_{I_r E} \le \Upsilon_e, \cap \left\{\Upsilon_{TI_r} \ge \Upsilon_t\right\} \middle| P_T\right\}}_{\mathscr{H}_1} \underbrace{\Pr\left\{\cap \left\{\Upsilon_{TI_k} < \Upsilon_t\right\} \middle| P_T\right\}}_{\mathscr{H}_2}. \tag{B.1}$$

The term $\mathscr{H}_2$ can be derived in the same way as $\mathscr{R}$, resulting in

$$\begin{aligned}\mathscr{H}_2 &= \left(\underbrace{\Pr\left\{\Upsilon_{TI_k} < \Upsilon_t \middle| P_T\right\}}_{\mathscr{Z}}\right)^{|\bar{\Delta}|} \\ &= \left(1 - e^{-\Upsilon_t V \wedge_I / P_T \eta_{TI}}\right)^{|\bar{\Delta}|} = \left(1 - e^{-\Upsilon_t V \wedge_I / P_T \eta_{TI}}\right)^{N - |\Delta|}.\end{aligned} \tag{B.2}$$

$\Upsilon_{I_r E}$ correlates Υ_{TI_r} because g_{TI_r} is their common term. Therefore, the term $\mathscr{H}_1$ must be rewritten in terms of

conditional probabilities as

$$\begin{aligned}\mathscr{H}_1 &= \Xi_{\{g_{TI_r}\}_{\mathrm{I}_r\in\Delta}}\left\{\Pr\left\{\min_{\mathrm{I}_r\in\Delta}\Upsilon_{I_rE}\le\Upsilon_e,\bigcap_{\mathrm{I}_r\in\Delta}\{\Upsilon_{TI_r}\ge\Upsilon_t\}\middle|P_T,\{g_{TI_r}\}_{\mathrm{I}_r\in\Delta}\right\}\right\}\\ &= \Xi_{\{g_{TI_r}\}_{\mathrm{I}_r\in\Delta}}\left\{\Pr\left\{\min_{\mathrm{I}_r\in\Delta}\Upsilon_{I_rE}\le\Upsilon_e\middle|P_T,\left\{g_{TI_r}\ge\frac{\Upsilon_t\widehat{V}_I}{P_T}\right\}_{\mathrm{I}_r\in\Delta}\right\}\right\}\\ &= \Xi_{\{g_{TI_r}\}_{\mathrm{I}_r\in\Delta}}\left\{1-\Pr\left\{\min_{\mathrm{I}_r\in\Delta}\Upsilon_{I_rE}>\Upsilon_e\middle|P_T,\left\{g_{TI_r}\ge\frac{\Upsilon_t\widehat{V}_I}{P_T}\right\}_{\mathrm{I}_r\in\Delta}\right\}\right\}\\ &= \Xi_{\{g_{TI_r}\}_{\mathrm{I}_r\in\Delta}}\{1\}-\Xi_{\{g_{TI_r}\}_{\mathrm{I}_r\in\Delta}}\left\{\prod_{\mathrm{I}_r\in\Delta}\Pr\left\{\Upsilon_{I_rE}>\Upsilon_e|P_T,g_{TI_r}\ge\frac{\Upsilon_t\widehat{V}_I}{P_T}\right\}\right\}\\ &= \Xi_{\{g_{TI_r}\}_{\mathrm{I}_r\in\Delta}}\{1\}-\prod_{\mathrm{I}_r\in\Delta}\Xi_{g_{TI_r}}\left\{\Pr\left\{\Upsilon_{I_rE}>\Upsilon_e|P_T,g_{TI_r}\ge\frac{\Upsilon_t\widehat{V}_I}{P_T}\right\}\right\}\\ &= \underbrace{\Xi_{\{g_{TI_r}\}_{\mathrm{I}_r\in\Delta}}\{1\}}_{\tilde{\mathscr{H}}_1}-\left(\underbrace{\Xi_{g_{TI_r}}\left\{\underbrace{\Pr\left\{\Upsilon_{I_rE}>\Upsilon_e|P_T,g_{TI_r}\ge\frac{\Upsilon_tV\wedge_I}{P_T}\right\}}_{\mathscr{I}}\right\}}_{\bar{\mathscr{H}}_1}\right)^{|\Delta|}.\end{aligned} \tag{B.3}$$

The term $\tilde{\mathscr{H}}_1$ is straightforwardly inferred as

$$\begin{aligned}\tilde{\mathscr{H}}_1 &= \prod_{\mathrm{I}_r\in\Delta}\Xi_{g_{TI_r}}\left\{1|g_{TI_r}\ge\frac{\Upsilon_t\widehat{V}_I}{P_T}\right\}\\ &= \prod_{\mathrm{I}_r\in\Delta}\int_{\Upsilon_t\widehat{V}_I/P_T}^{\infty}f_{g_{TI_r}}(x)dx=\left(e^{-\Upsilon_tV\wedge_I/P_T\eta_{TI}}\right)^{|\Delta|}\\ &= e^{-\Upsilon_tV\wedge_I|\Delta|/P_T\eta_{TI}}.\end{aligned} \tag{B.4}$$

In order to compute $\bar{\mathscr{H}}_1$, the term $\mathscr{I}$ is firstly derived after inserting the explicit form of Υ_{I_rE} in (15) into (B.3) as

$$\begin{aligned}\mathscr{I} &= \Pr\left\{\Upsilon_{I_rE}>\Upsilon_e\middle|P_T,g_{TI_r}\ge\frac{\Upsilon_t\widehat{V}_I}{P_T}\right\}\\ &= \Pr\left\{\frac{g_{I_rE}\bar{P}_{I_r}}{V_E}>\Upsilon_e\middle|P_T,g_{TI_r}\ge\frac{\Upsilon_t\widehat{V}_I}{P_T}\right\}\\ &= \Xi_{\bar{P}_{I_r}}\left\{e^{-\Upsilon_eV_E/\bar{P}_{I_r}\eta_{IE}}\middle|P_T,g_{TI_r}\ge\frac{\Upsilon_t\widehat{V}_I}{P_T}\right\}.\end{aligned} \tag{B.5}$$

Plugging (16) into (B.5), the compact form of $\mathscr{I}$ is obtained as

$$\begin{aligned}\mathscr{I} &= \Xi_{g_{I_rR}}\left\{e^{-\Upsilon_eV_E/\eta_{IE}\min\left(\frac{Q_p}{g_{I_rR}},P_{I_r}\right)}\middle|P_T,g_{TI_r}\ge\frac{\Upsilon_t\widehat{V}_I}{P_T}\right\}\\ &= \int_{Q_p/P_{I_r}}^{\infty}e^{-\Upsilon_eV_E/\eta_{IE}Q_px}\frac{1}{\eta_{IR}}e^{-x/\eta_{IR}}dx\\ &\quad+\int_0^{Q_p/P_{I_r}}e^{-\Upsilon_eV_E/\eta_{IE}P_{I_r}}\frac{1}{\eta_{IR}}e^{-x/\eta_{IR}}dx=(S-1)e^{-U/P_{I_r}}\\ &\quad+e^{-H/P_{I_r}},\end{aligned} \tag{B.6}$$

where U, S, and H are given in (31), (32), and (33), correspondingly.

Inserting (B.6) into $\bar{\mathscr{H}}_1$ results in

$$\begin{aligned}\bar{\mathscr{H}}_1 &= (S-1)\underbrace{\Xi_{g_{TI_r}}\left\{e^{-U/P_{I_r}}\middle|P_T,g_{TI_r}\ge\frac{\Upsilon_t\widehat{V}_I}{P_T}\right\}}_{\mathscr{K}(U,P_T)}\\ &\quad+\underbrace{\Xi_{g_{TI_r}}\left\{e^{-H/P_{I_r}}\middle|P_T,g_{TI_r}\ge\frac{\Upsilon_t\widehat{V}_I}{P_T}\right\}}_{\mathscr{K}(U,P_T)}.\end{aligned} \tag{B.7}$$

Given P_{I_r} in (4), the function $\mathscr{K}(n,P_T)$ is simplified as

$$\begin{aligned}\mathscr{K}(n,P_T) &= \Xi_{g_{TI_r}}\left\{e^{-n/P_Tg_{TI_r}M+L}\middle|P_T,g_{TI_r}\ge\frac{\Upsilon_t\widehat{V}_I}{P_T}\right\}\\ &= \int_{\Upsilon_t\widehat{V}_I/P_T}^{\infty}e^{-n/P_TMx+L}\frac{1}{\eta_{TI}}e^{-x/\eta_{TI}}dx.\end{aligned} \tag{B.8}$$

By the variable change $y=x+(L/P_TM)$, one rewrites $\mathscr{K}(n,P_T)$ as

$$\mathscr{K}(n,P_T)=\frac{e^{L/\eta_{TI}P_TM}}{\eta_{TI}}\int_{(\Upsilon_t\widehat{V}_I+L/M)/P_T}^{\infty}e^{-\frac{n}{P_TM}/y-y/\eta_{TI}}dy. \tag{B.9}$$

By defining

$$\mathscr{G}(c,v,b)=\int_c^{\infty}e^{-v/y-by}dy, \tag{B.10}$$

it is apparent that (B.9) coincides (35). Accordingly, the proof continues with showing that the function $\mathscr{G}(c,v,b)$ is presented in the precise closed form as (34). Toward this end, one applies the series expansion to $e^{-b/y}$, which results in

$$\mathscr{G}(c,v,b)=\int_c^{\infty}\left[\sum_{m=0}^{\infty}\frac{1}{m!}\left(-\frac{v}{y}\right)^m\right]e^{-by}dy=\sum_{m=0}^{\infty}\frac{(-v)^m}{m!}\int_c^{\infty}\frac{e^{-by}}{y^m}dy. \tag{B.11}$$

By the variable change $x=by$, one rewrites $\mathscr{G}(c,v,b)$ as

$$\mathscr{G}(c,v,b)=\sum_{m=0}^{\infty}\frac{(-vb)^m}{m!b}\int_{cb}^{\infty}\frac{e^{-x}}{x^m}dx. \tag{B.12}$$

With the help of [63], eq. (3.381.6), the last integral in (B.12) is expressed in closed-form in terms of the Whittaker function; hence, (B.12) exactly matches (34).

Plugging (B.4) and (B.7) into (B.3) and then inserting the result together with (B.2) into (B.1), one achieves

$$\begin{aligned}\mathscr{H} &= \left[e^{-\Upsilon_tV\wedge_I|\Delta|/P_T\eta_{TI}}-\{(S-1)\mathscr{K}(U,P_T)+\mathscr{K}(H,P_T)\}^{|\Delta|}\right]\\ &\quad\cdot\left(1-e^{-\Upsilon_tV\wedge_I/P_T\eta_{TI}}\right)^{N-|\Delta|}.\end{aligned} \tag{B.13}$$

Because $\mathscr{W} = \Xi_{P_T}\{\mathscr{H}\}$ and $P_T = \min\left(\left(Q_p/g_{TR}\right), P_p\right)$, by replacing P_T with $\min\left(\left(Q_p/g_{TR}\right), P_p\right)$ in the formula of $\mathscr{H}$ and averaging $\mathscr{H}$ over the random variable g_{TR}, one obtains the single-integral formula of $\mathscr{W}$ as (29). As such, the proof is completed.

Data Availability

The authors declare that all data used to support the findings of this study are included within the article.

Conflicts of Interest

The authors declare that they have no conflicts of interest.

Acknowledgments

This research is funded by the Vietnam National Foundation for Science and Technology Development (NAFOSTED) under grant number 102.04-2019.318. We would like to thank Ho Chi Minh City University of Technology (HCMUT), VNU-HCM, for the support of time and facilities for this study.

References

[1] W. S. H. M. W. Ahmad, N. A. M. Radzi, F. S. Samidi et al., "5G Technology: Towards Dynamic Spectrum Sharing Using Cognitive Radio Networks," *IEEE Access*, vol. 8, pp. 14460–14488, 2020.

[2] A. Alqasir and A. E. Kamal, "Cooperative Small Cell HetNets with Dynamic Sleeping and Energy Harvesting," *IEEE Transactions on Green Communications and Networking*, p. 1, 2020.

[3] K. Shafique, B. A. Khawaja, F. Sabir, S. Qazi, and M. Mustaqim, "Internet of things (IoT) for next-generation smart systems: a review of current challenges, future trends and prospects for emerging 5G-IoT scenarios," *IEEE Access*, vol. 8, pp. 23022–23040, 2020.

[4] M. J. Sobouti, Z. Rahimi, A. H. Mohajerzadeh et al., "Efficient deployment of small Cell Base stations mounted on unmanned aerial vehicles for the internet of things infrastructure," *IEEE Sensors Journal*, vol. 20, no. 13, pp. 7460–7471, 2020.

[5] Y. Dai and L. Lyu, "NOMA-Enabled CoMP clustering and power control for green internet of things networks," *IEEE Access*, vol. 8, pp. 90109–90117, 2020.

[6] F. Benkhelifa, H. ElSawy, J. A. Mccann, and M. Alouini, "Recycling cellular energy for self-sustainable IoT networks: a spatiotemporal study," *IEEE Transactions on Wireless Communications*, vol. 19, no. 4, pp. 2699–2712, 2020.

[7] FCC, *Spectrum policy task force report*, ET Docket 02−135, 2002.

[8] M. Polese, M. Giordani, T. Zugno et al., "Integrated access and backhaul in 5G mmWave networks: potential and challenges," *IEEE Communications Magazine*, vol. 58, no. 3, pp. 62–68, 2020.

[9] I. Dey, D. Ciuonzo, and P. S. Rossi, "Wideband Collaborative Spectrum Sensing using Massive MIMO Decision Fusion," *IEEE Transactions on Wireless Communications*, p. 1, 2020.

[10] L. Ge, G. Chen, Y. Zhang, J. Tang, J. Wang, and J. A. Chambers, "Performance analysis for multihop cognitive radio networks with energy harvesting by using stochastic geometry," *IEEE Internet of Things Journal*, vol. 7, no. 2, pp. 1154–1163, 2020.

[11] S. Buzzi, I. Chih-Lin, T. E. Klein, H. V. Poor, C. Yang, and A. Zappone, "A Survey of Energy-Efficient Techniques for 5G Networks and Challenges Ahead," *IEEE Journal on Selected Areas in Communications*, vol. 34, no. 4, pp. 697–709, 2016.

[12] D. Feng, C. Jiang, G. Lim, L. J. Cimini, G. Feng, and G. Y. Li, "A survey of energy-efficient wireless communications," *IEEE Communications Surveys & Tutorials*, vol. 15, no. 1, pp. 167–178, 2013.

[13] A. Celik, A. Alsharoa, and A. E. Kamal, "Hybrid Energy Harvesting Cooperative Spectrum Sensing in Heterogeneous CRNs," in *2016 IEEE Globecom Workshops (GC Wkshps)*, vol. 4−8, pp. 1–6, Washington DC, USA, 2017.

[14] X. Lu, P. Wang, D. Niyato, D. I. Kim, and Z. Han, "Wireless networks with RF energy harvesting: a contemporary survey," *IEEE Communications Surveys & Tutorials*, vol. 17, no. 2, pp. 757–789, 2015.

[15] L. Xu, W. Yin, X. Zhang, and Y. Yang, "Fairness-Aware Throughput Maximization over Cognitive Heterogeneous NOMA Networks for Industrial Cognitive IoT," *IEEE Transactions on Communications*, p. 1, 2020.

[16] G. Xu, C. Yang, J. Wu, and C. Chang, "Harvesting electromagnetic energy in air: a wireless energy harvester at 2.45 GHz using inexpensive materials," *IEEE Microwave Magazine*, vol. 21, no. 6, pp. 88–95, 2020.

[17] F. Zhou, Z. Li, J. Cheng, Q. Li, and J. Si, "Robust AN-aided Beamforming and power splitting Design for Secure MISO cognitive radio with SWIPT," *IEEE Transactions on Wireless Communications*, vol. 16, no. 4, pp. 2450–2464, 2017.

[18] G. Pan, H. Lei, Y. Yuan, and Z. Ding, "Performance analysis and optimization for SWIPT wireless sensor networks," *IEEE Transactions on Communications*, vol. 65, no. 5, pp. 2291–2302, 2017.

[19] T. Liu, X. Wang, and L. Zheng, "A cooperative SWIPT scheme for wirelessly powered sensor networks," *IEEE Transactions on Communications*, vol. 65, no. 6, pp. 2740–2752, 2017.

[20] H. Ding, D. B. da Costa, H. A. Suraweera, and J. Ge, "Role Selection Cooperative Systems With Energy Harvesting Relays," *IEEE Transactions on Wireless Communications*, vol. 15, no. 6, pp. 4218–4233, 2016.

[21] Y. Gu and S. Aissa, "RF-Based energy harvesting in decode-and-forward relaying systems: Ergodic and outage capacities," *IEEE Transactions on Wireless Communications*, vol. 14, no. 11, pp. 6425–6434, 2015.

[22] A. Rajaram, D. N. K. Jayakody, K. Srinivasan, B. Chen, and V. Sharma, "Opportunistic-Harvesting: RF wireless power transfer scheme for multiple access relays system," *IEEE Access*, vol. 5, pp. 16084–16099, 2017.

[23] A. Hamani, B. Allard, T.-P. Vuong, M. C. E. Yagoub, and R. Touhami, "Design of Rectenna Series-association Circuits for radio frequency energy harvesting in CMOS FD-SOI 28 nm," *IET Circuits, Devices & Systems*, vol. 12, no. 1, pp. 40–49, 2018.

[24] K. Janghel and S. Prakriya, "Performance of secondary network with primary Beamforming-assisted energy harvesting transmitters," *IEEE Transactions on Vehicular Technology*, vol. 66, no. 10, pp. 8895–8909, 2017.

[25] M. R. Amini and M. W. Baidas, "Availability-Reliability-Stability trade-offs in ultra-reliable energy-harvesting cognitive radio IoT networks," *IEEE Access*, vol. 8, pp. 82890–82916, 2020.

[26] M. Babaei, U. Aygolu, M. Basaran, and L. Durak-Ata, "BER Performance of Full-Duplex Cognitive Radio Network with

Nonlinear Energy Harvesting," *IEEE Transactions on Green Communications and Networking*, vol. 4, no. 2, pp. 448–460, 2020.

[27] A. Paul and S. P. Maity, "Outage analysis in cognitive radio networks with energy harvesting and Q-routing," *IEEE Transactions on Vehicular Technology*, vol. 69, no. 6, pp. 6755–6765, 2020.

[28] M. Hayashi and A. Vazquez-Castro, "Two-Way Physical Layer Security Protocol for Gaussian Channels," *IEEE Transactions on Communications*, vol. 68, no. 5, pp. 3068–3078, 2020.

[29] F. Zhu and M. Yao, "Improving Physical-Layer security for CRNs using SINR-based cooperative Beamforming," *IEEE Transactions on Vehicular Technology*, vol. 65, no. 3, pp. 1835–1841, 2016.

[30] I. Krikidis and B. Ottersten, "Secrecy sum-rate for orthogonal random Beamforming with opportunistic scheduling," *IEEE Signal Processing Letters*, vol. 20, no. 2, pp. 141–144, 2013.

[31] S. Yan, N. Yang, R. Malaney, and J. Yuan, "Transmit antenna selection with Alamouti coding and power allocation in MIMO wiretap channels," *IEEE Transactions on Wireless Communications*, vol. 13, no. 3, pp. 1656–1667, 2014.

[32] I. Krikidis, J. Thompson, and S. Mclaughlin, "Relay selection for secure cooperative networks with jamming," *IEEE Transactions on Wireless Communications*, vol. 8, no. 10, pp. 5003–5011, 2009.

[33] B. He and X. Zhou, "Secure on-off transmission design with channel estimation errors," *IEEE Transactions on Information Forensics and Security*, vol. 8, no. 12, pp. 1923–1936, 2013.

[34] J.-H. Lee, "Full-duplex relay for enhancing physical layer security in multi-hop relaying systems," *IEEE Communications Letters*, vol. 19, no. 4, pp. 525–528, 2015.

[35] K. Ho-Van, "Outage analysis in cooperative cognitive networks with opportunistic relay selection under Imperfect Channel information," *AEU - International Journal of Electronics and Communications*, vol. 69, no. 11, pp. 1700–1708, 2015.

[36] H. T. Nguyen, S. Q. Nguyen, and W.-J. Hwang, "Performance Analysis of Energy Harvesting Relay Systems under Unreliable Backhaul Connections," *IET Communications*, vol. 12, no. 15, pp. 1763–1770, 2018.

[37] C. Yin, H. T. Nguyen, C. Kundu, Z. Kaleem, E. Garcia-Palacios, and T. Q. Duong, "Secure Energy Harvesting Relay Networks with Unreliable Backhaul Connections," *IEEE Access*, vol. 6, pp. 12074–12084, 2018.

[38] H. T. Nguyen, J. Zhang, N. Yang, T. Q. Duong, and W.-J. Hwang, "Secure Cooperative Single Carrier Systems under Unreliable Backhaul and Dense Networks Impact," *IEEE Access*, vol. 5, pp. 18310–18324, 2017.

[39] K. Ho-Van and T. Do-Dac, "Analysis of security performance of relay selection in underlay cognitive networks," *IET Communications*, vol. 12, no. 1, pp. 102–108, 2018.

[40] K. Ho-Van, T. Do-Dac, N. Pham-Thi-Dan et al., "Improving Information Security in Cognitive Radio Networks with Relay Selection," in *Proc. ISEE*, vol. 29-30, pp. 274–279, HCM City, Vietnam, 2017.

[41] P. Maji, B. Prasad, S. D. Roy, and S. Kundu, "Secrecy outage of a cognitive radio network with selection of energy harvesting relay and imperfect CSI," *Wireless Personal Communications*, vol. 100, no. 2, pp. 571–586, 2018.

[42] F. Benkhelifa and M. S. Alouini, "A Thresholding-based Antenna Switching in MIMO Cognitive Radio Networks with SWIPT-enabled Secondary Receiver," in *2017 IEEE International Conference on Communications (ICC)*, vol. 21–25, pp. 1–6, Paris, France, May 2017.

[43] T. D. Hieu, T. T. Duy, and S. G. Choi, "Performance Enhancement for Harvest-to-Transmit Cognitive Multi-hop Networks with Best Path Selection Method under Presence of Eavesdropper," in *Proc. IEEE ICACT, GW*, vol. 11–14, pp. 323–328, Korea, February 2018.

[44] X. Zhang, J. Xing, Z. Yan, Y. Gao, and W. Wang, "Outage Performance Study of Cognitive Relay Networks with Imperfect Channel Knowledge," *IEEE Communications Letters*, vol. 17, no. 1, pp. 27–30, 2013.

[45] M. Seyfi, S. Muhaidat, and J. Liang, "Relay selection in cognitive radio networks with interference constraints," *IET Communications*, vol. 7, no. 10, pp. 922–930, 2013.

[46] K. Ho-Van, "Influence of channel information imperfection on outage probability of cooperative cognitive networks with partial relay selection," *Wireless Personal Communications*, vol. 94, no. 4, pp. 3285–3302, 2017.

[47] X. Zhou, R. Zhang, and C. K. Ho, "Wireless information and power transfer: architecture design and rate-energy tradeoff," *IEEE Transactions on Communications*, vol. 61, no. 11, pp. 4754–4767, 2013.

[48] A. A. Nasir, X. Zhou, S. Durrani, and R. A. Kennedy, "Relaying protocols for wireless energy harvesting and information processing," *IEEE Transactions on Wireless Communications*, vol. 12, no. 7, pp. 3622–3636, 2013.

[49] P. M. Quang, T. T. Duy, and V. N. Q. Bao, "Performance Evaluation of Underlay Cognitive Radio Networks over Nakagamim fading Channels with Eenergy Harvesting," in *Proc. IEEE ATC*, vol. 10–12, pp. 108–113, HaNoi, Vietnam, October 2016.

[50] J. Zhang, G. Pan, and H. M. Wang, "On physical-layer security in underlay cognitive radio networks with full-duplex wireless-powered secondary system," *IEEE Access*, vol. 4, pp. 3887–3893, 2016.

[51] W. Mou, W. Yang, X. Xu, X. Li, and Y. Cai, "Secure Transmission in Spectrum-Sharing Cognitive Networks with Wireless Power Transfer," in *Proc. IEEE WCSP*, vol. 13–15, pp. 1–5, JiangSu, China, October 2016.

[52] H. Lei, M. Xu, H. Zhang, G. Pan, I. S. Ansari, and K. A. Qaraqe, "Secrecy Outage Performance for Underlay MIMO CRNs with Energy Harvesting and Transmit Antenna Selection," in *Proc. IEEE Globecom*, vol. 4–8, pp. 1–6, Washington DC, USA, December 2016.

[53] A. Singh, M. R. Bhatnagar, and R. K. Mallik, "Secrecy outage of a simultaneous wireless information and power transfer cognitive radio system," *IEEE Wireless Communications Letters*, vol. 5, no. 3, pp. 288–291, 2016.

[54] Y. Liu, L. Wang, S. A. R. Zaidi, M. Elkashlan, and T. Q. Duong, "Secure D2D communication in large-scale cognitive cellular networks: a wireless power transfer model," *IEEE Transactions on Communications*, vol. 64, no. 1, pp. 329–342, 2016.

[55] S. Raghuwanshi, P. Maji, S. D. Roy, and S. Kundu, "Secrecy Performance Of a Dual Hop Cognitive Relay Network with an Energy Harvesting Relay," in *Proc. IEEE ICACCI*, vol. 21–24, pp. 1622–1627, Jaipur, India, September 2016.

[56] R. Su, Y. Wang, and R. Sun, "Destination-Assisted Jamming for Physical-Layer Security in SWIPT Cognitive Radio Systems," in *Proc. IEEE WCNC*, vol. 15-18, pp. 1–6, Barcelona, Spain, April 2018.

[57] H. Lei, M. Xu, I. S. Ansari, G. Pan, K. A. Qaraqe, and M.-S. Alouini, "On secure underlay MIMO cognitive radio

networks with energy harvesting and transmit antenna selection," *IEEE Transactions on Green Communications and Networking*, vol. 1, no. 2, pp. 192–203, 2017.

[58] Z. Ning, L. Ning, C. Nan, J. W. Mark, and S. Xuemin, "Cooperative Networking towards Secure Communications for CRNs," in *Proc. IEEE WCNC*, vol. 7-10, pp. 1691–1696, Shanghai, China, April 2013.

[59] A. Bletsas, A. Khisti, D. P. Reed, and A. Lippman, "A simple cooperative diversity method based on network path selection," *IEEE Journal on Selected Areas in Communications*, vol. 24, no. 3, pp. 659–672, 2006.

[60] A. Mukherjee and A. L. Swindlehurst, "Detecting Passive Eavesdroppers in The MIMO Wiretap Channel," in *Proc. IEEE ICASSP*, pp. 2809–2812, Kyoto, Japan, 2012.

[61] M. Zhang, K. Cumanan, J. Thiyagalingam et al., "Energy efficiency optimization for secure transmission in MISO cognitive radio network with energy harvesting," *IEEE Access*, vol. 7, pp. 126234–126252, 2019.

[62] K. Ho-Van, "Exact outage probability analysis of proactive relay selection in cognitive radio networks with MRC receivers," *Journal of Communications and Networks*, vol. 18, pp. 288–298, 2016.

[63] I. S. Gradshteyn and I. M. Ryzhik, *Table of Integrals, Series and Products*, Academic, San Diego, CA, 6th edition, 2000.